

VIBRATORY PENETRATION AND FLOW SHEARING IN GRANULAR MATERIALS: A REVIEW OF PERSPECTIVES

VIBROFONCAGE ET CISAILLEMENT D'ÉCOULEMENT DES MATERIAUX GRANULAIRES : EXAMEN DE PERSPECTIVES

Alain Holeyman¹ and Louis Michiels¹

¹ Department of Civil and Environmental Engineering – University of Louvain, Louvain-la-Neuve, Belgium

ABSTRACT – The present paper reviews our current fundamental and engineering abilities to assess vibro-drivability, i.e. predicting the vibratory penetration log of a given pile into a given soil profile using a given vibrator. Testing undertaken to provide insight into the pile-soil-vibrator interaction and its modelling is then emphasized. Degradation of the skin friction upon cyclic shear stress can be evaluated by applying elements of earthquake engineering practice used to assess liquefaction potential. Several available methods to explore the flow-like behaviour of sheared granular materials are reviewed. Our present ability to assess the vibratory capacity of a pile from the monitoring of its vibratory performance is critically reviewed. Finally, suggestions for further research, design and practice are provided.

RÉSUMÉ – Le présent article passe en revue les connaissances fondamentales et appliquées permettant d'estimer le vibrofonçage, c'est-à-dire la pénétration vibratoire d'un pieu donné dans un profil de sol donné en utilisant un vibreur donné. Les essais entrepris pour éclaircir l'interaction sol-pieu et sa modélisation sont spécifiquement étudiés. La dégradation de la friction à l'interface sous un cisaillement cyclique peut être évaluée en appliquant des éléments développés dans le cadre du génie parasismique et notamment le potentiel de liquéfaction. Plusieurs méthodes disponibles pour explorer le comportement des milieux granulaires sous cisaillement, comparable à un écoulement, sont passés en revue. Notre capacité actuelle à estimer la capacité vibratoire d'un pieu à partir du suivi instrumenté de ses performances vibratoires est décrite et critiquée. Enfin, des suggestions sont introduites pour la recherche future, la conception et la mise en œuvre.

1. Introduction

The behaviour of soil subjected to vibratory loading is complex in several regards: soil is a geometrically complex assemblage of solid grains of various sizes and shapes leaving room for void conferring it its porous character (Figure 1a). Voids can be filled with water, air (or soil vapour), or both. Mechanically speaking, soil is considered by many as a solid-like medium inasmuch normal and deviatoric stresses can be assumed by the soil matrix, or skeleton. The loads transferred through the inter-particles contacts can be described in terms of “effective stresses”, using the well-accepted soil mechanics concept introduced by Terzaghi in 1926.

When a *densely* packed cohesionless soil is subjected to shearing, its overall skeleton volume tends to expand, as originally shown by Reynolds (1885), see Figure 1b. Conversely, when a *loosely* packed cohesionless soil is subjected to cyclic loading, its overall skeleton volume tends to shrink. If the soil is dry, that tendency is directly expressed by volume decrease of the soil.

If on the other hand the soil is *saturated* and the cyclic loading takes place at a pace that exceeds consolidation processes, thereby preventing volume reduction, that tendency is expressed by an increase in the pore water pressure. Upon reaching the total stress, the pore pressure essentially takes over control of the mixture behaviour, while the effective stress vanishes. At that point the soil transforms into a grain suspension and loses its solid-like

mechanical properties: this ultimate degradation is called *liquefaction*. Furthermore, cohesionless materials cannot take any tension at interparticle contacts, leaving the pore fluid as the only medium able to resist that effect. Soil vapour or bubbles may originate when the tensile stress exceeds the *cavitation* suction of the pore fluid.

When *dry* soils are subjected to rapid shearing, they can expand from their initial packing into a looser state, as shown in Figure 1a (dilute condition) where grains are no longer in continuous contact with their neighbours. An average effective stress may still exist in a statistical sense, expressing the intensity of the particles interactions within this agitated grain cloud, similar to that of a Brownian movement.

In order to understand the magic associated with vibratory compaction or vibratory driving, one would ideally have to master several fields of physics and mechanics under both macroscopic and microscopic scales: soil mechanics, hydraulics, rheology, tribology, granular mechanics and sedimentology, just to mention a few. Although numerous scientists have contributed to the various fields that will be reviewed in this paper, it is fair to admit that we have not, at this time, really understood all the fundamental aspects of vibrocompaction and vibrodriving. There is therefore a need for knowledge to advance in that field. That does not prevent engineers and practitioners to benefit from the magic, but sometimes also to suffer from unsuccessful attempts on construction sites.

Although the paper will address the onset of liquefaction of soils and fluidization of granular materials, it will mainly focus on the fundamentals and experimental observations pertaining to material flow, keeping an eye on rate effects, i.e. characterizing the dependence of the shear stress upon the shearing rate. For that matter, we will generally prefer the approach of imposed deformations to that of imposed stresses.

2. Soil Mechanics perspective

2.1. Fundamentals

As the pile undergoes a vibratory vertical motion of amplitude s , it communicates to the lateral neighboring soil shear stresses and shear strains, as sketched in Figure 2. It is also forcing normal and potentially convective movement of soil below the pile toe. As those mechanisms govern soil resistance along the shaft and at the toe, the understanding of the shear stress/shear strain relationship, i.e. $\tau(\gamma)$, within the soil becomes of paramount importance.

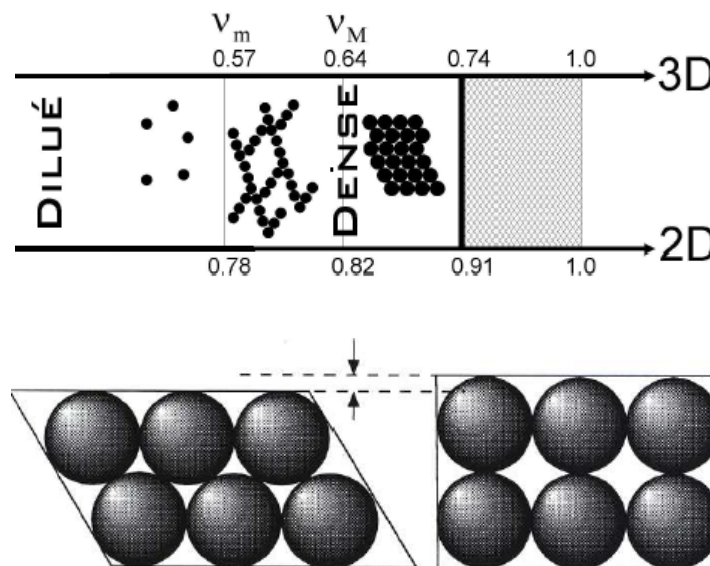


Figure 1. (a) Skeleton and voids of granular states, (b) Dilatancy of dense packing (after DaCruz, 2004)

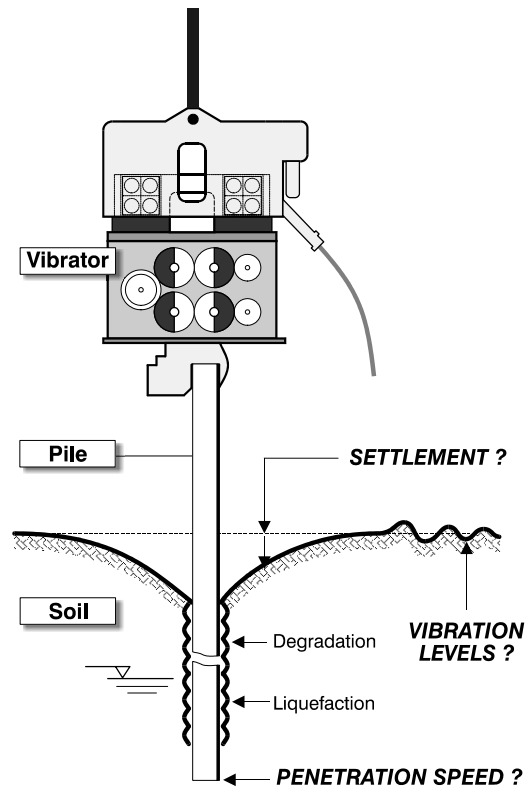


Figure 2. Effects of vibrating profile on neighbouring soil

That aspect of soil behaviour has been more extensively studied within the field of earthquake engineering, leading to the characterization of so-called constitutive relationships, generally on the basis of laboratory testing of soil samples (mainly triaxial testing and simple shear testing).

The constitutive relationships that represent the complex large-strain, dynamic and cyclic shear stress-strain strength behaviour of the medium surrounding the vibrating profile require the characterization of the following elements :

- Static stress-strain law expressing non-linear behaviour under monotonic loading and hysteresis upon strain reversal,
- Shear modulus at small strains and ultimate shear strength,
- Softening and increase of hysteretic damping with increasing strain,
- Effect of strain rate on initial shear modulus and ultimate strength,
- Degradation of properties resulting from the application of numerous cycles, and last but not least,
- Generation of excess pore pressure leading to substantial loss of resistance and possibly to liquefaction.

The following paragraphs address key components of the constitutive relationships and provide insight on the intrinsic soil behaviour in the vicinity of the vibrating profile

2.2. Static and Cyclic Stress-strain Behaviour

A typical soil response to uniform cyclic strains with amplitude γ_c is represented in Figure 3, which highlights the following fundamental parameters:

G_{max} : initial (or tangent) shear modulus

τ_c : shear stress mobilized at γ_c

G_s : secant (or equivalent) shear modulus

ι : hysteretic (or intrinsic) damping ratio;

$$\iota = \Delta W / 2\pi\gamma_c\tau_c \quad (1)$$

with ΔW = Energy lost during a given cycle.

Both G_s and ι are strain-dependent parameters that need to be described by specific laws within a given cycle. τ_{max} is the ultimate shear strength, revealed at large strains. τ_{max} and G_{max} are shown to decrease with the number of cycles (cyclic degradation).

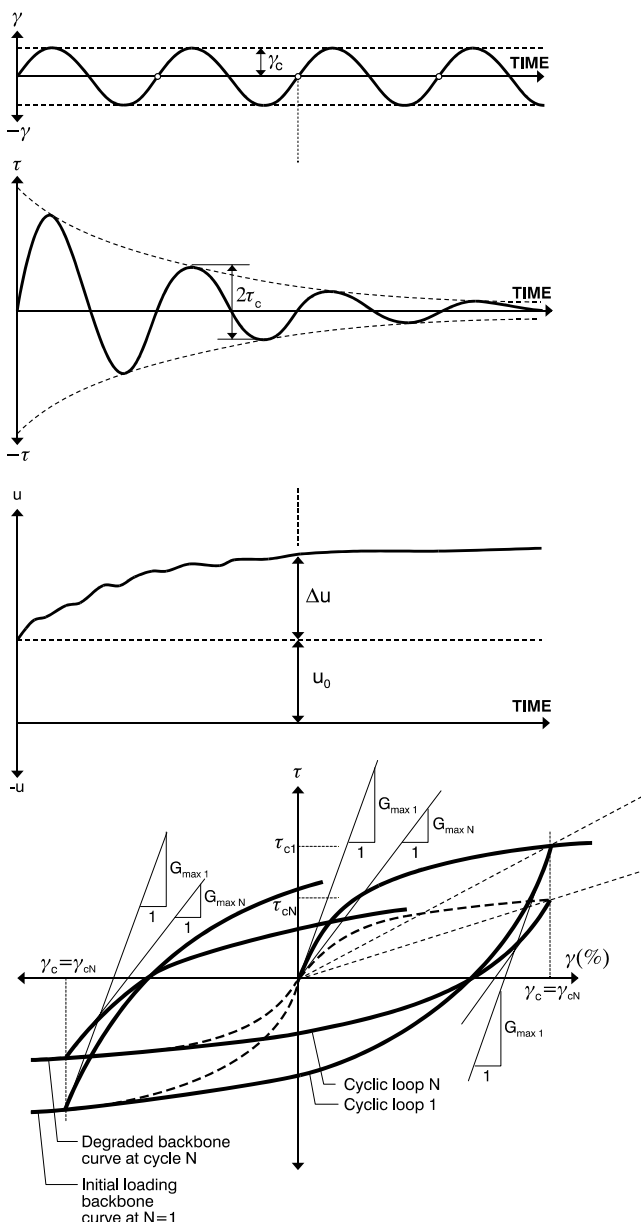


Figure 3. Soil Behavior under Constant Cyclic Shear Strain Amplitude Loading (From Vucetic, 1993; 1994)

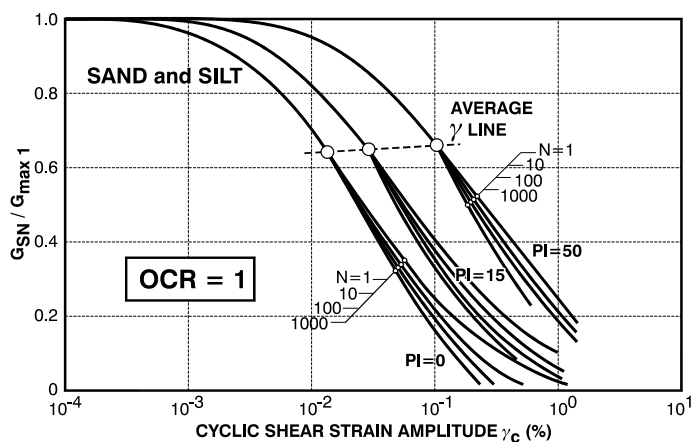


Figure 4. Soil stiffness degradation resulting from cyclic shear (Vucetic, 1993)

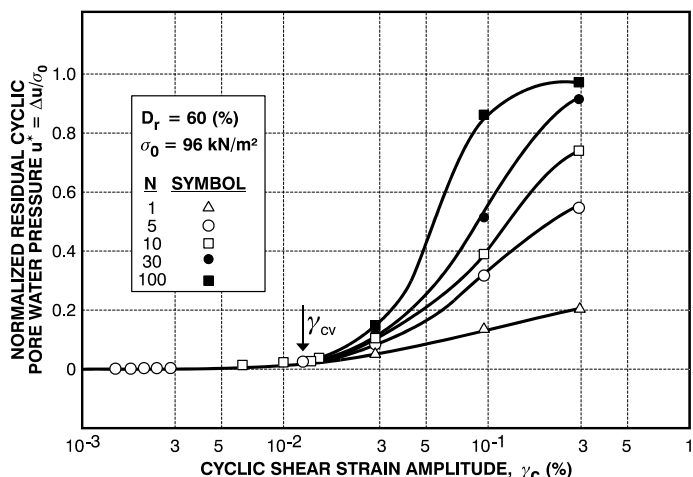


Figure 5. Build up of residual pore pressure in different sands in undrained cyclic strain-controlled tests (Dobry et al., 1982)

2.3. Initial Shear modulus and ultimate shear strength (G_{max} and τ_{max})

Numerous studies have dealt with the initial shear modulus to be used in earthquake engineering (e.g. Drnevich et al., 1967). Most of them are supported by parameters determined in the laboratory which are generally not available when a vibratory penetration issue arises. However, correlations with CPT test results have been developed (Seed and De Alba, 1986, Robertson and Wride, 1998)

2.4. Secant Shear Modulus and Hysteretic Damping (G_s and ι)

As can be observed in Figure 3, G_s decreases with the shear strain during the initial monotonic loading. The curve that represents the initial monotonic loading is referred to as the initial

"backbone" curve, because it also serves as the basis to generate the family of curves corresponding to unloading and reloading. Kondner's mathematical formulation (1963) is frequently employed to describe the initial backbone curve in earthquake engineering. That hyperbolic law is best represented in terms of reduced variables, η , the mobilization ratio and δ , the relative shear :

$$\eta = \tau / \tau_{\max} = \delta / (\delta + 1) \quad (2)$$

with $\delta = \gamma / \gamma_r = \gamma \cdot G_{\max} / \tau_{\max}$ (3)

and $\gamma_r = \tau_{\max} / G_{\max}$ (4)

γ_r is called the reference strain. Two of the three parameters G_{\max} , γ_r , and τ_{\max} , are generally derived from laboratory experiments. More recent laboratory research by Vanden Berghe (1999) points towards the upward curvature of the stress/strain curve at large cyclic strains. From the point of maximum straining, the unloading curve is described by the following equation, in accordance with Masing's rules 1 and 2 (Masing, 1926):

$$\tau = \tau_0 (\gamma - \gamma_0) / (1/G_{\max} + (\gamma - \gamma_0) / 2\tau_{\max}) \quad (5)$$

The energy dissipated within a loop depends for a given soil on the amplitude of the cyclic strain. Empirical data collected in laboratory tests indicates that the damping ratio increases with γ_c as the soil undergoes higher plastic deformations. Dobry and Vucetic (1987, Vucetic & Dobry 1991, and Vucetic 1993 & 1994) have suggested a unifying approach to accommodate the influence of the nature of the material characterized by the plasticity index (PI), as indicated in Figure 4.

2.5. Strain Rate Effects

Although it has been identified that undrained modulus and shear strength increase with increasing shear straining rate ($\dot{\gamma} = \partial\gamma / \partial t$ or "strain rate" for short), experimental data generated using different apparatuses and loading conditions lead to different conclusions. Viscosity mechanisms may well provide a suitable framework to understand the strain rate effect observed when comparing fast and slow undrained monotonic stress-strain curves, as well as to explain the roundness of the loop tips during a sinusoidal strain-controlled cyclic test. Evidence would point to the fact that sands and non plastic silts have very small viscosity in that their stress-strain loops exhibit sharp rather than rounded tips (Dobry and Vucetic, 1987).

The mathematical functions proposed in the literature to represent the nonlinear viscosity also depend on the type of experimental observations. A power law is often adopted:

$$\tau_{kin} = \tau_{sta} \cdot (1 + J \cdot \dot{\gamma}^n) \quad (6)$$

with τ_{kin} = kinetic ultimate shear strength [kPa]
 τ_{sta} = "static" ultimate shear strength [kPa]
 $\dot{\gamma}$ = shear strain rate [s^{-1}]

The advantage of that mathematical form is that resistance does not vanish as the strain rate goes to zero. The power law also requires the strain rate to vary by orders of magnitude to provide tangible increases in both the modulus and the ultimate strength. The J coefficient and n exponent depend on the nature of the soil.

Based on pile driving data, $n=0.2$ and $J=0.3 s^{-0.2}$ have been suggested for plastic soils. J should therefore essentially depend on the plasticity of the soil, with several authors believing it to be quite limited for granular materials.

2.6. Assessment of soil “damping” to interpret load tests

Damping was introduced as a first approximation by Smith (1960) to account for some velocity dependency of the mobilized soil resistance during dynamic loading (see Figure 16). For nearly half a century, an overwhelming majority of papers dealing with dynamic load tests have been published without questioning the validity of that framework. While offering the benefit of simplicity and conceptual ease of understanding, correlations with soil type remained unconvincing, specially in finer grained materials to the point that site specific calibration of dynamic test has been requested in many circumstances by the skeptical practicing engineers. Furthermore, various definitions of damping have added to the confusion: Smith-type (original), Smith viscous, and Case dampings, just to name the three main ones. Then came more mathematically involved definitions of damping such as those suggested by Gibson (1968) and by Rausche et al. (1994).

Clarification of what constitutes damping has been progressively developed by few researchers (e.g. Holeyman, 1984, Paquet, 1988, El Naggar & Novack, 1994, Randolph & Deeks, 1992, as summarized in Figures 7 and 8). It has now been established that energy losses result from geometric damping, from soil intrinsic damping, and that steady-state resistance depends upon failure rate.

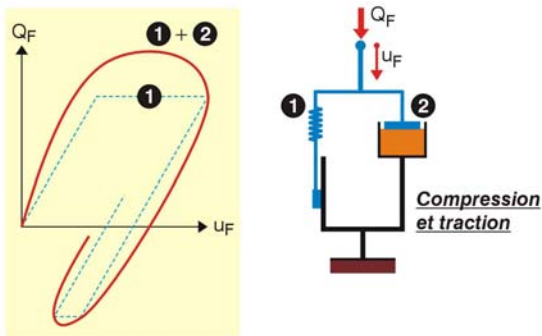


Figure 6. Basic form of damping (Smith, 1960)

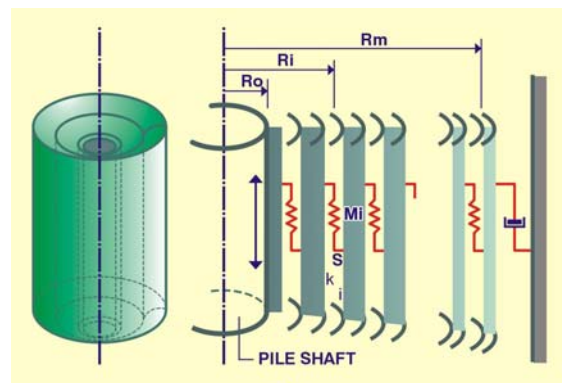


Figure 7. Skin friction radial modeling (Holeyman, 1984)

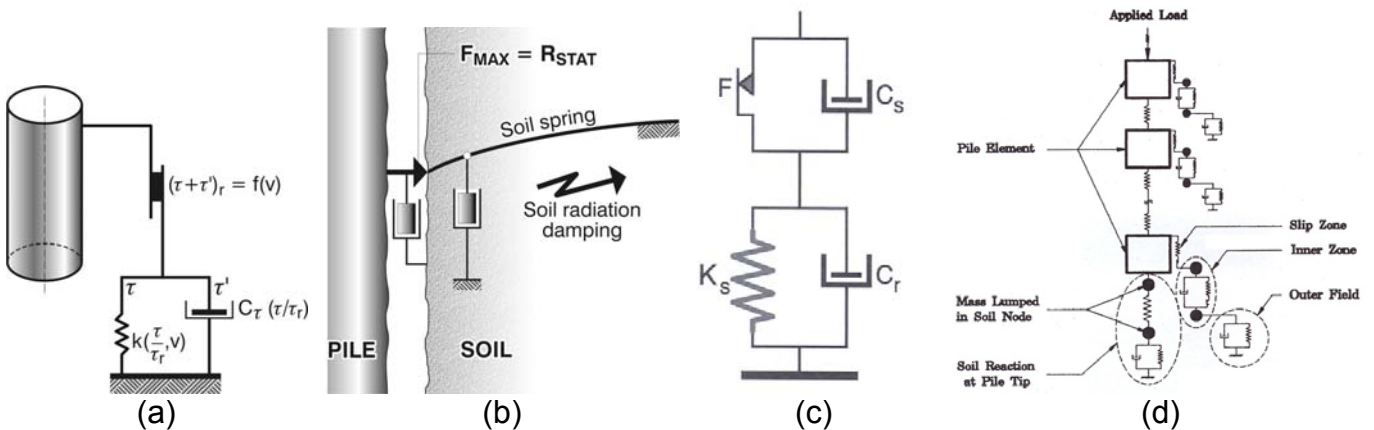


Figure 8. Soil-Pile dynamic interaction Models : (a) Holeyman, 1984, (b) Paquet, 1988 (c) Randolph & Deeks, 1992, (d) El Naggar & Novak, 1994

Geometric damping accounts for energy dissipation into the elastic medium surrounding the pile. The intrinsic damping itself accounts for energy losses due to viscosity at low strains and due to non-recoverable behavior (hysteretic damping) at higher strains. Finally, the term “failure damping” is suggested here as a simplified term to describe the velocity dependence of the steady-state resistance. In spite of the now available conceptual and physically based

developments, simplicity of the all encompassing damping “J factor” is still being preferred by the vast majority of the practicing pile testers.

2.7. Failure “damping” or steady rate effect

On the other hand, research at the University of Sheffield has recently produced encouraging results from laboratory tests conducted in a calibration chamber that clarify the velocity dependence of the steady-state or Constant Rate of Penetration (CRP) resistance of a model pile jacked at different penetration rates into clay beds as shown in Figure 9. Brown (2006) and Anderson et al. (2006) present variations of a progressively activated damping, the ultimate value of which follows a power-type function as initially suggested by Gibson :

$$\frac{\tau_d}{\tau_s} = 1 + \alpha \left(\frac{\tau_d}{\tau_{d(ultimate)}} \right) \left(\frac{v_d}{v_s} \right)^{0.2} \quad (7)$$

where τ_d is the dynamic shear resistance, τ_s is the assumed static shear resistance determined at a pile velocity of 0.01mm/s, $\tau_{d(ultimate)}$ is the ultimate dynamic shear resistance, v_d is the pile velocity, v_s is the assumed static pile velocity which is 0.01mm/s in that study.

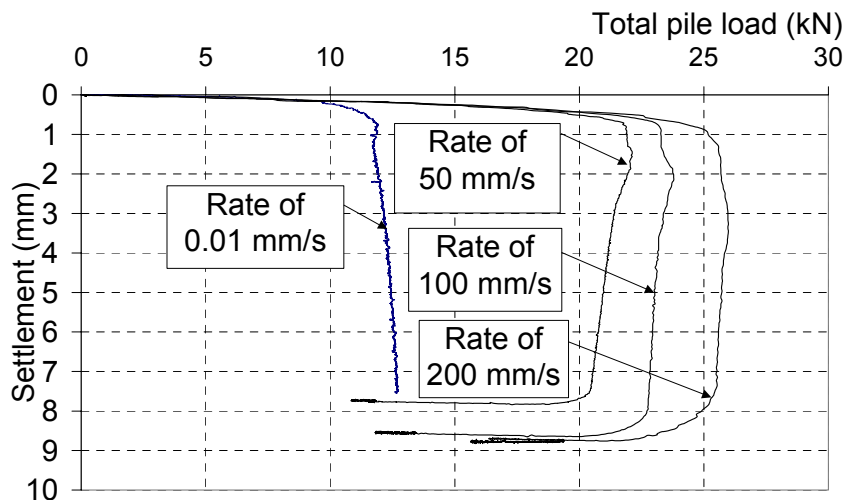


Figure 9. Model Pile Load-settlement curves at different penetration rates (Anderson et al, 2006)

These recent results should however be confronted to experimental and numerical results produced by Randolph and co-workers (2005) pertaining to the penetration of cones or T-bars, newly developed for offshore geotechnical exploration of soft clays. According to those researchers, the monotonic increase of the resistance can only be observed under an undrained assumption for the soil behavior, shown on Figure 10. If on the contrary, allowance is made for consolidation, the resistance increases again at lower penetration rates. This implies that a lower bound penetration resistance can be found at intermediate penetration rates, as shown on Figure 11.

These latter results may well question the validity of the quest for the “true” or “unique” load-settlement curve advocated by Fleming (1992) and England (1993). That noteworthy development is indeed based on fitting hyperbolic functions to settlement data measured during a 2 to 6 hours accurately maintained load.

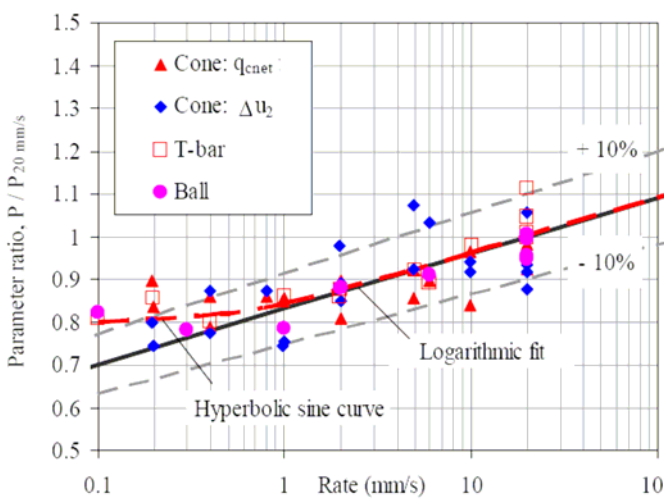


Figure 10. Effect of penetration rate on undrained resistance (Randolph, 2004)

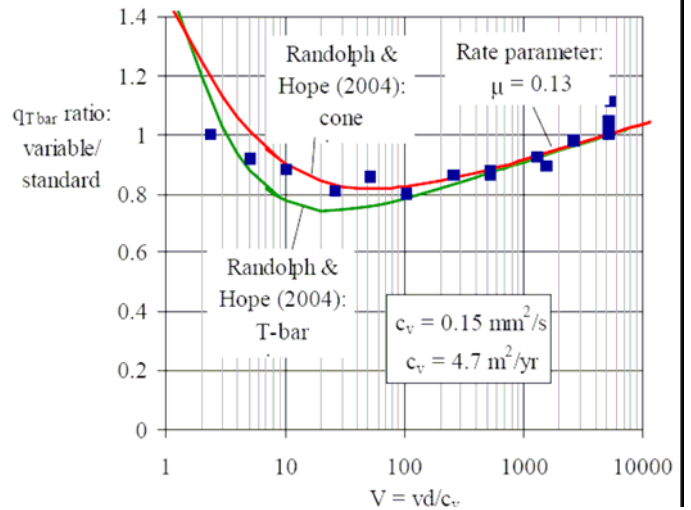


Figure 11. Penetration resistance from T-bar "twitch" tests (Randolph, 2005)

2.8. Degradation Law

When subjected to undrained cyclic loading involving a number N of large strain cycles, the soil structure continuously deteriorates, the pore pressure increases, and the secant shear modulus decreases with N . This process known as *cyclic stiffness degradation* can be best characterized on the basis of strain controlled tests for the type of loading involved with the vibratory penetration of piles. Typical results of strain-controlled tests are sketched in Figure 4, where the degradation is clearly expressed by the decrease of the amplitude of the peak stress mobilized at successive cycles.

The quantification of the degradation process calls for the introduction of the degradation index Δ , defined by:

$$\tau_n = \Delta \cdot \tau_1 \quad (8)$$

Laboratory results conducted at constant cyclic strain show that in many soils, the degradation index after N cycles can be approximated by the following relationship as suggested by Idriss et al (1978):

$$\Delta = N^{-t} \quad (9)$$

The exponent t , called degradation parameter, depends mainly on the amplitude of the cyclic strain and the nature of the material (PI), as suggested by Dobry and Vucetic (1988) and as indicated in Figure 4 Vucetic, 1993). It is noteworthy that the degradation parameter assumes a zero value at strains smaller than a cyclic "threshold" shear strain, γ_{cv} . The threshold strain increases with the plasticity of the soil, as suggested in Figure 4.

2.9. Soil liquefaction

Vibration induced compaction of saturated sands has received attention not only from the earthquake engineering community, but also from vibro-compaction specialists. Recent advances tend to indicate that build up of pore pressures (eventually leading to liquefaction) and volume reduction of cyclically loaded materials are the expression of the same phenomenon, i.e. the irreversible tendency for loose to medium dense particulate arrangements to achieve a denser packing when sheared back and forth.

Under drained conditions, the volume reduction is immediate. Under undrained conditions, the tendency for volume reduction is expressed by an increase in the pore water pressure (see Figure 5), such that the effective stress is reduced to a value that may be close to zero. It is then necessary to wait for the soil to consolidate in order to see the volume reduction take

place.

The strain-driven evaluation of the build up of pore pressure as suggested by Dobry et al. (1979) is an approach that lends itself to a direct transposition to the problem of the vibrations induced by a vertically vibrating pile. It also allows one to evaluate potential changes of the void ratio based on a cyclic strain rather than stress history, as supported by laboratory drained tests conducted on sands by Youd (1972). That framework of analysis enhanced by the threshold cyclic strain concept embodies in a single model the intrinsic relationship between degradation and pore pressure build-up, with the advantage that it can be applied to general categories of soils (sands to clays)

The excess pore pressure generated during cyclic loading has been shown (see Figure 5) to increase with the shear strain and the number of cycles for a given soil type. The damage parameter κ approach (Finn, 1981) can be adopted to evaluate the excess pore pressure δu resulting from a particular strain history.

3. Experimental perspective from pile vibratory driving

The above discussion of soil behaviour under cyclic loading does not encompass the particular geometry of the profile-soil interface, nor does it consider the continuous penetration of the profile that leads to successive exploration stages into “virgin” soil behaviour. That is why a number of experiments have been conducted to reveal soil-structure interaction within a vibratory framework. Based on the ambition and complexity of the tested interface, one can categorize various experiences reported in the literature as conceptual, interface, and both reduced and full-scale testing.

3.1. Conceptual model testing

Tests have been conducted by several Russian researchers to investigate the “vibro-viscous” resistance of soils. In particular, Barkan (1963) reports on the sphere test, shown in Figure 12a, where a steel ball is sunk into a vibrated soil vessel with the assistance of a bias force. Penetration speed is shown to obey Stokes sedimentation law (see Figure 12b), allowing him to determine an equivalent viscosity μ . The inverse of that equivalent kinematic viscosity [cm.s/kg] was shown to vary linearly with the relative level of acceleration (a/g), passed a threshold value of approximately 1.4 for a dry sand (see Figure 12c). The influence of the water content on the “vibro-viscosity factor $1/\mu$ ” of a sand vibrated at constant a/g is also shown in Figure 12d, highlighting the nearly total loss of vibro-penetrability at water contents corresponding to the optimal Proctor compaction test leading to the maximum density.

3.2. Pile-soil interface testing

Soil shear strength resisting the pulling out of a vibrating steel plate against a normal stress controlled medium sand (vibratory direct shear box) has been investigated in the early days by Levchinsky and Savtchencko (Barkan, 1963). The friction coefficient ($\tan \phi = \tau/\sigma$) was shown to decrease with cyclic amplitude and frequency. The ultimate relative reduction of the friction was also shown to increase with the grain size within the investigated range shown in Figure 13. That figure shows indeed that the sand vibratory friction angle can easily drop to $1/2$ to $1/5$ of its static value.

3.3. Reduced scale tests

Testing of model profiles in soil tanks were initially attempted by Bernhard (1968), Schmid and Hill (1966), continued by Rodger and Littlejohn (1980), Billet and Siffert (1985) and O'Neill et al (1990), and more recently by Viking (1998), Holeyman et al (1999), and Canou et al. (2005).

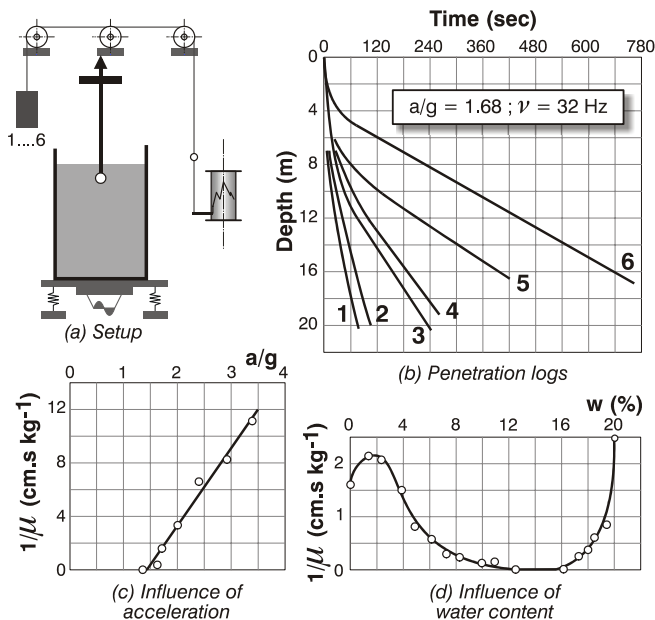


Figure 12. Sphere penetration experiments (after Barkan, 1963)

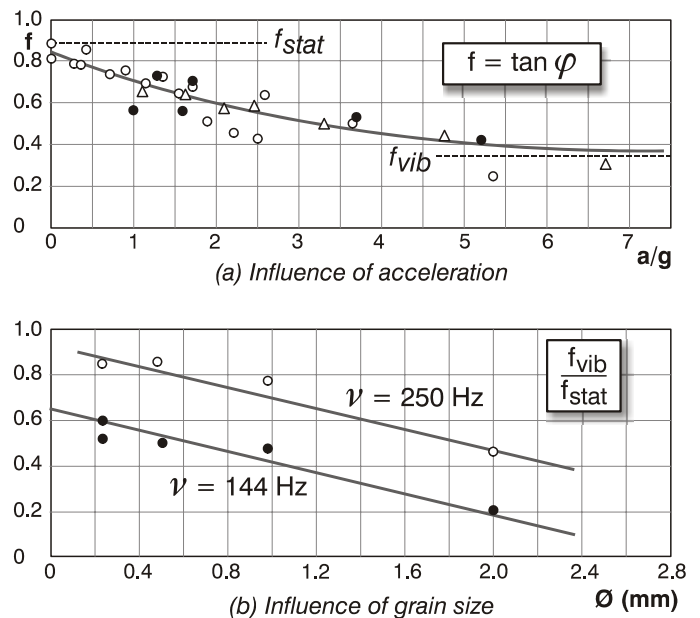


Figure 13. Vibratory friction of sand (after Levchinsky and Savtchencko, as reported by Barkan, 1963)

The tests were generally conducted using a lightweight vibrator acting on a heavily instrumented profile. Monitoring included strain gauges, accelerometers and displacement transducers. The soil used was exclusively sand (dry, moist, or saturated), placed at a controlled density, and in some cases, confined at a controlled radial stress. Monitoring of the soil response involved accelerometers, total stress and pore pressure cells during installation as well as compaction and in situ testing after installation.

Insightful observations relative to the vibratory toe resistance have been reported by Schmid (1966), who identified three regimes, depending on the magnitude of the eccentric driving force

- a sinusoidal resistance domain, for a driving force lower than the "resistance threshold"
- an impact domain, when the upward force exceeds the soil uplift resistance; the toe of the pile alternately separates from the soil and tamps it
- a phase instability domain, when the downward stationary force exceeds the soil compressive resistance.

Rodger and Littlejohn (1980) call upon acceleration amplitude of the vibrating profile to distinguish :

- the elastic state ($a < 0.6g$)
- the trans-threshold state ($0.6g < a < 1.5g$), wherein most of the shear strength reduction takes place,
- the fluidized response state ($a > 1.5g$).

Although their views are contradicted by some of Barkan's observations, these three different states are stated to be confirmed by dynamic direct shear tests performed by others. Results of tank experiments have been reported in terms of friction reduction coefficients, potential optimal operation, and have shed some light on fundamental soil behavior.

Correlations have been established between penetration speed and parameters induced by the vibrator (amplitude, frequency) and by the soil (grain size, relative density, and lateral stress). Although conclusions of the tests conducted under different conditions do not consistently agree, those experiments *generally* identified that :

- penetration speed increased when the relative density decreased and the bias mass increased
- friction was reduced to 30 to 50% of its static value, while a more limited reduction was noted for the toe resistance
- optimum operation of the hammer required at times that the frequency or eccentric moment be reduced, while energy transfer was of the order of 40% of the full theoretical power produced by the vibrator

- a number of observations cannot be explained.

Although reduced scale models are of use, they mostly suffer from improper boundary conditions (at the tank limits) that significantly prevent the vibration energy from propagating away from its source.

3.4. Full scale tests

Because of inconsistencies in the conclusions derived from reduced scale tests, research has been conducted in several countries based on full-scale tests. Early full-scale programmes have been conducted by Barkan (1963) and Davisson (1970). Other programmes have been conducted by manufacturers on specific equipment, but lead to a limited diffusion of their conclusions. More recently, collective European programs have provided actual penetration speed, but within soil conditions that cannot be controlled, only characterized. Monitoring nowadays involves acceleration, strain, pore pressure, penetration speed, making the tested profile a fully instrumented probe. Such programs have produced results that have not been fully analyzed (BBRI, 1994, Sipdis, 1997); others have been more completely interpreted (KTH, 1999, IREX, 2000-2006). Publication of such detailed research results are extensively appreciated by both the profession and the fundamental researchers.

3.5. Apparent resonance

Holeyman (1993b) has suggested to use of a radial discrete model to calculate the vertical shear waves propagating away from the pile. The model, shown in Figure 14, consists in a succession of concentric cylinders with a linearly increasing depth. The equations of movement are integrated for each cylinder based on their dynamic shear equilibrium in the vertical direction, in a manner similar to that used by Smith (1960) in the longitudinal direction.

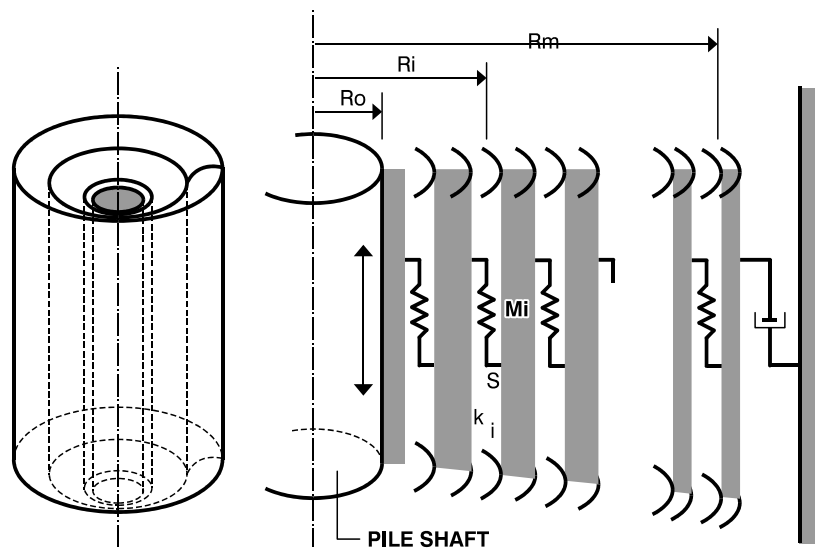


Figure 14. Radial 1-D model (Holeyman, 1993b)

The model allows the constitutive relationships described in the first paragraphs of this section to be readily deployed. The major advantage of that shear wave propagation model is to closely follow the development of degradation as more cycles are simulated. It can also provide insight into vibration levels in the vicinity of the pile. Both features are illustrated by Figure 15 which provides the effective particle velocity calculated at several distances away from a profile upon vibrator start up. An apparent resonance is indicated, whereas the model does not include a longitudinal or radial dimension that could explain the frequency at which the peak vibration is noted : why? Simply because the model most probably reproduces two soil-pile interaction vibratory modes: the coupled mode and the uncoupled mode.

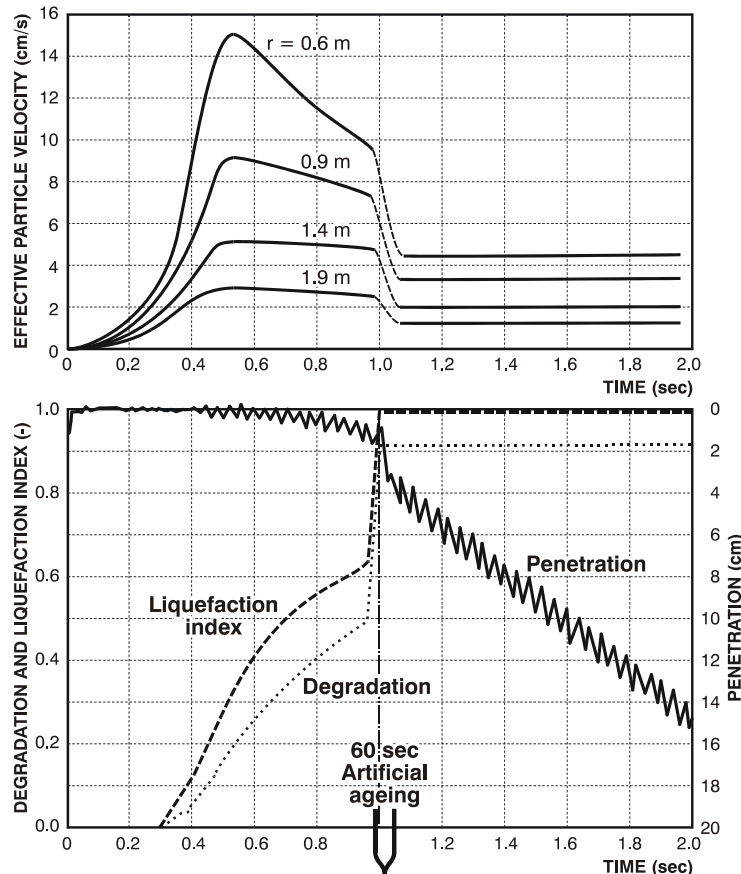


Figure 15. Vibration levels and penetration state parameters estimated upon vibrator start-up and regime

In the coupled mode (similar to Schmid's sinusoidal domain), the soil remains in contact with the slowly vibrating profile, and the transfer of energy from the pile to the soil is nearly perfect. As the vibrator constantly accelerates between 0 and 0.5 seconds, vibration levels tend to increase with the square of time since start up. However, as the soil begins to degrade, its shear modulus decreases and the specific shear impedance reduces, leading to loss in the energy transfer. At that point, the coupling between soil and pile suffers some slippage, and therefore time lag. After a sufficient number of cycles, the soil has significantly degraded, and has entered into liquefaction after 60 seconds (ageing skipped in Figure 15).

As the shear modulus of the soil in contact with the profile is nearly zero, very little energy can pass through the fluidized surrounding zone. The soil in the vicinity of the profile cannot anymore follow the profile movement, from which it uncouples itself, resulting in a lower level of vibration. That example demonstrates that apparent resonance of soil vibration may be no more than the transient combination of increased rotation speed and soil degradation. The model can also shed light on "damping" as it clearly separates geometric damping from the energy losses attributable to viscous and hysteretic behaviour.

3.6. Bearing capacity from vibratory site monitoring

Because soil resistance degradation is significant during vibratory driving, one should expect it a challenge to estimate the static bearing capacity from the end of penetration vibratory performance of a driven profile.

In the impact driving practice, it is recognized that end of driving (EOD) data generally provides a safe estimate of the pile capacity; that is why beginning of restrrike (BOR) or "retap" data is strongly advised to the owner who wishes to tap the value of letting the soil set up. If the end of Vibratory driving (EOV) data is used, methods to estimate the static capacity should allow for recovery of soil degradation. However significant uncertainty should be expected in

the process because the inverse of observed degradation coefficients may range between 2 and 10.

That is why extreme caution is warranted when applying so-called pile Vibratory driving (PVD), formulae, even more so than already much detracted (impact) pile driving formulae. A limited number of such PVD formulae have been published; however only one (the so-called "Snipe" formula) has, to the author's knowledge been extensively field tested.

4. Granular flows

4.1. Introduction

The study of granular flows has picked up momentum in the last 20 years as computing power has become more readily available. Some conditions are generally required to facilitate granular flows: a rather low relative density is welcome and either complete or nil saturation. Physicists are devoting significant efforts in the physical and numerical modelling of such flowing media. The behaviour of a liquid loaded with grains is addressed in the case of a saturated condition, while the behaviour of dense granular flow is addressed in the case of a dry condition. Several key problems pertaining to the manufacturing, combustion, military, agronomy, food, and pharmaceutical industries have been solved thanks to those recent advances.

As the studied material is subject to phase transformations (solid, liquid, and gas-like behaviour), different disciplines have been looking at various declinations of the same class of problems. As a result, different concepts, definitions, and approaches appear further away than they truly are. After a review of governing parameters and dimensionless variables while thriving to bridge the gap between soil mechanics and physics, different flow regimes will be identified and characterized through either experimental or numerical modelling.

4.2. Density

Granular flows addressed in physics mostly concern monodisperse media, i.e. consisting of spheres of a uniform diameter (d). This allows more idealized definitions of density related variables. Bagnold (1954) used the "linear concentration" $\lambda = d/s$, with s being the free distance (or net spacing) between spheres. The volume concentration (C) is then the ratio of the grain occupied space to the whole space, similar to GDR MiDi (2004)'s definition of volume fraction (Φ). Soil mechanics uses more general void parameters, such as porosity (n), void ratio (e), water content (w), and soil related parameters, such as relative density (Dr), liquidity Index (Il), and critical density. Equivalences are provided below:

$$\phi = C = 1 - n = 1/(1 + e) = Co(1/\lambda + 1)^{-3} \quad (10)$$

Co is the maximum possible concentration ($s = 0$), which is equal to $\pi/\sqrt{18} = 0.74$ for spheres arranged in a tetrahedral-rectangular piling (see Figure 1). That maximum concentration needs to be reduced to allow relative shear by one layer of spheres overriding the adjacent one. Bagnold expects general shearing to become possible when λ reduces to a value of 12 to 14, or C gets below 0.60, or when soil mechanics's porosity n exceeds 40% and void ratio 0.7.

4.2. Stresses

Since soil is at least a two-phase medium, it has been possible to identify stress components corresponding to each phase, thanks to the effective stress principle introduced by Terzaghi in 1926:

$$\sigma'_{ij} = \sigma_{ij} - u \quad (11)$$

The (macroscopic) effective stress components governing the behaviour of the soil skeleton can be obtained by subtracting the isotropic pore fluid pressure u from the total (measurable) stress. That effective stress is similar to Bagnold “dispersive pressure” expressing the macroscopic tendency for the suspended grains to disperse. The more dilatant the behaviour, the higher the dispersive pressure.

4.2. Flow concepts

Flow can occur as a particular form of movement or deformation not only within gases and liquids, but also within pastes as well as granular solids. As a result of the various phases involved (solid grains, air, and water), the mechanisms can be quite complex, sometimes abruptly transitioning from solid to gas, no unified description allows one at the present time to deal with all types of behaviour described below.

Physicists use several dimensionless parameters, listed below, to quantify the relative importance of inertia, velocity, pressure, friction, stiffness, and viscosity:

$$I = \dot{\gamma} d / \sqrt{P / \rho} \quad (12) \quad \text{inertia vs. pressure,}$$

with P =pressure and ρ =bulk density

$$\mu = \tau / \sigma \quad (13) \quad \text{friction coefficient}$$

$$T_i = \tau / (\rho d^2 \dot{\gamma}^2) \quad (14) \quad \text{Inertial shear stress}$$

$$T_k = \tau d / k \quad (15) \quad \text{Elastic shear stress,}$$

with k = inter-particle stiffness

$$\Theta = k / (\rho d^3 \dot{\gamma}^2) \quad (16) \quad \text{Elastic vs. inertial shear stress}$$

$$N = \sqrt{\lambda} \rho_s d^2 \dot{\gamma} / \eta \quad (17) \quad \text{Inertial vs. viscous stress,}$$

with $\eta = \tau / \dot{\gamma}$, dynamic viscosity

4.3. Quasi-static regime

In soil mechanics, “critical state” is defined as a condition in which plastic shearing can continue indefinitely, *without changes in volume or effective stresses*. Under prolonged shearing, soil tends to reach that critical state as to minimize energy dissipation. When the soil is saturated and rapidly loaded, like during vibratory loading, undrained behaviour has to be considered since the pore water has not enough time to escape from the rapidly loaded soil volume. It is noteworthy that the critical density corresponding to the attainment of the critical state depends on the means effective stress $p' = (\sigma'_1 + \sigma'_2 + \sigma'_3) / 3$, as shown for Brusselian sand in Figure 16 (Vanden Berghe, 2001).

Four types of soil behaviour can be observed during undrained triaxial tests. Each type is function of the combination between the void ratio e and the initial mean stress p_0' relatively to the critical void ratio line. Indeed, four zones can be identified on the graph of void ratio versus mean stress (Figure 16) and each zone corresponds to a type of behaviour when the deviator stress q increases:

- ZONE I: Contractive then dilative behaviour with a critical mean stress higher than the initial mean stress.
- ZONE IIa: Contractive then dilative behaviour with a critical mean stress smaller than the initial mean stress.
- ZONE II: Contractive behaviour with a non zero critical mean stress.
- ZONE III: Contractive with a zero critical mean stress (corresponding to static liquefaction).
- ZONE IV: Generally inaccessible zone under conventional soil mechanics ; higher void ratios can however be achieved under dynamic or flow conditions, as discussed herein.

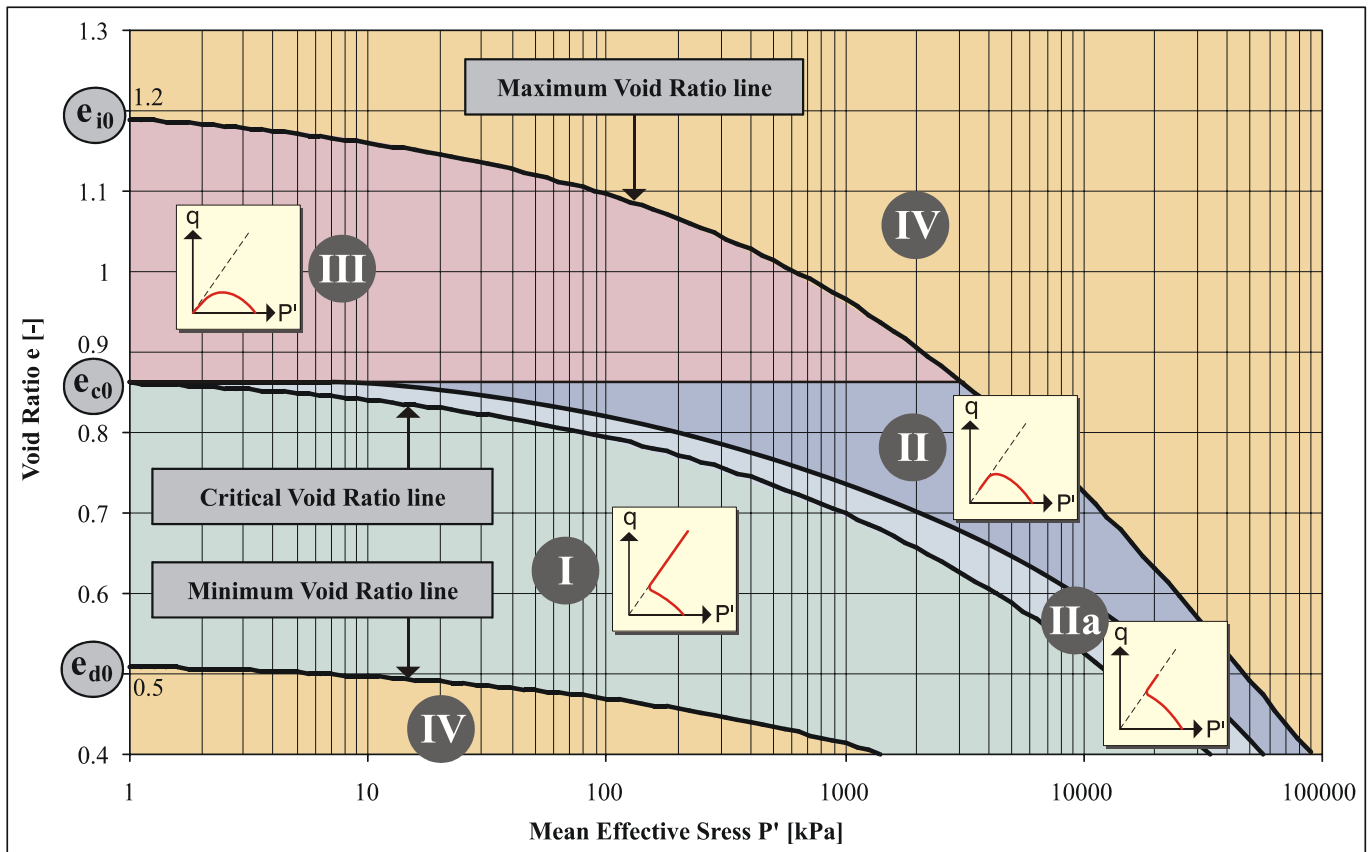


Figure 16. Brusselian sand behavior types in the critical states diagram (Vanden Berghe, 2001)

Soil plasticity models are generally used to cope with what the physicists call the “quasi-static” regime, characterized by negligible inertia effects and a limited strain rate. The mean shear straining rate has been defined with equation 8. Under the quasi-static regime, forces are transferred through interparticle contacts. The inter-particle forces are essentially maintained, without any noticeable dynamic effects: even though an evolution of the forces at individual contacts can be noted as the material is sheared, the force chains regenerates and macroscopic stresses remain overall stationary. It can also be observed that the concept and definition of the critical state avoids the use of time, and therefore, strictly speaking, it is implied that the shear straining rate does not influence the behaviour types defined by Figure 16, which may be viewed as a shortcoming of the critical state model.

4.4. Gaseous regime

The gaseous regime is observed in flows affecting dry cohesionless materials when the grains are strongly agitated and the grains are far apart from another, similar to the conditions that enabled the development of the kinetic theory of gases. That regime is also called collisional because the particles behaviour is governed by binary collisions, that are supposed to last a negligible fraction of their flight. Under the earth’s gravity, very large shear straining rates are required to maintain a rapid granular flow as the “granular temperature” must be large enough to generate sufficient “dispersive” pressure to support the weight of the material. A shear straining rate of 70 s^{-1} is mentioned in some experiments conducted by Wang & Campbell (1992). When the voids are occupied by a viscous fluid, even more extreme shear straining rates are required to observe an inertial behaviour of the “dispersion” (Bagnold, 1954).

5. Discrete Elements Modelling

5.1. Introduction

The behaviour of flows under a collisional regime can be calculated using Discrete Element Modelling, as originally suggested by Cundall & Stack (1979). A soft particle technique models the interaction between particles according to e.g. the mechanical idealization shown in Figure 17. It can be noted that besides the stiffness k introduced by equation (15), a dashpot is used to model the energy dissipation upon impact as to match the coefficient of restitution, while a local friction coefficient μ is used to account for particle roughness.

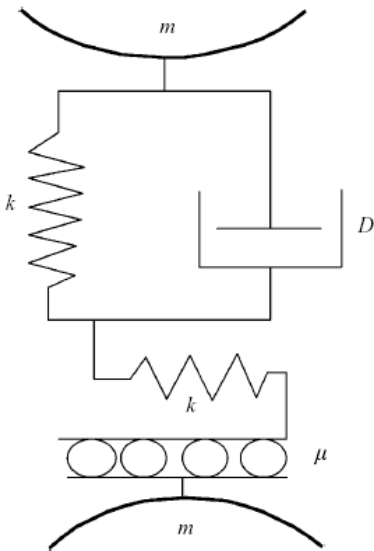


Figure 17. Schematic of a particle contact model

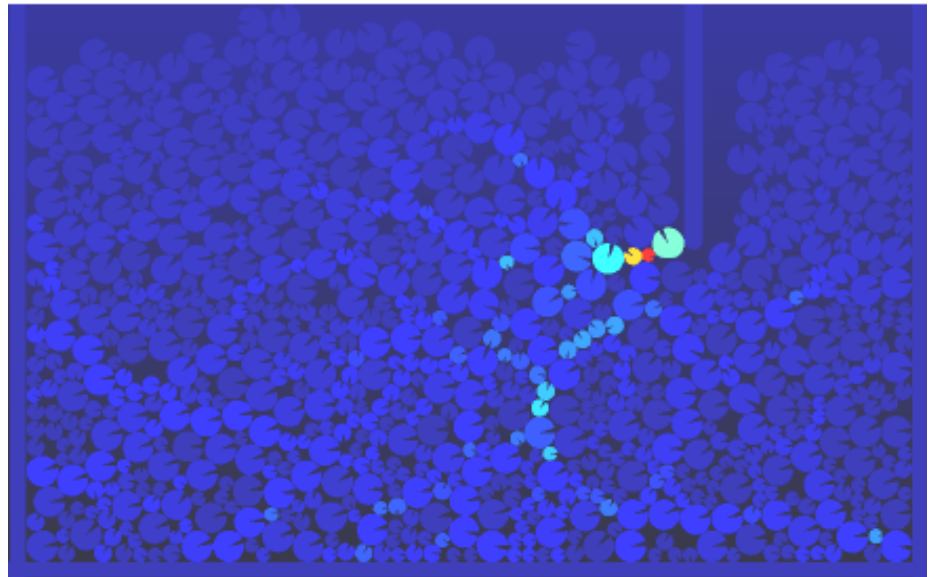


Figure 18. Mapping of force chains from DEM simulation of vibratory penetration (Deveugle & Mossoux, 2006)

2-D (disks) and 3-D (spheres) computer programs are available, but calculation times remain an obstacle to date in spite of the wide availability of ever more powerful computers. The reason lies in the numbers of particles to model a real-life problem. Simulations reported in publications generally confine themselves to the 1,000 to 20,000 particle range, which is not much when considering that there are more than 10,000 grains in 1 cm³ of Brussellian sand.

Results of a simulation of the penetration of a horizontally vibrating needle in a box containing disks are provided in Figure 18. The computer code LMGC90 (Jean, 1996 and Dubois, 2006) was recently used by Deveugle & Mossoux (2006) and visually enhanced using the Gmsh package (Gueuzaine & Remacle, 2001) to, amongst other, map the force chains such as those apparent on Figure 18. A 1.4GHz Intel Centrino based PC took 6 hours to calculate the simulation shown on Figure 18, which can be considered as a minimal configuration because involving only a 2-D simulation of approximately 1,000 disks. Basic mechanisms can be simulated under much simplified geometry and limited number of particles, but one can hope that within 10 to 30 years, modelling of millions of particles may come within reach.

5.2 Recent numerical and physical modelling

The French research group GDR-MiDi has summarized comprehensive results from both experimental and numerical modelling of monodisperse spheres. The main results applicable to the confined conditions shown on Figure 19, prevailing under vibratory driving and compaction, are reviewed hereunder.

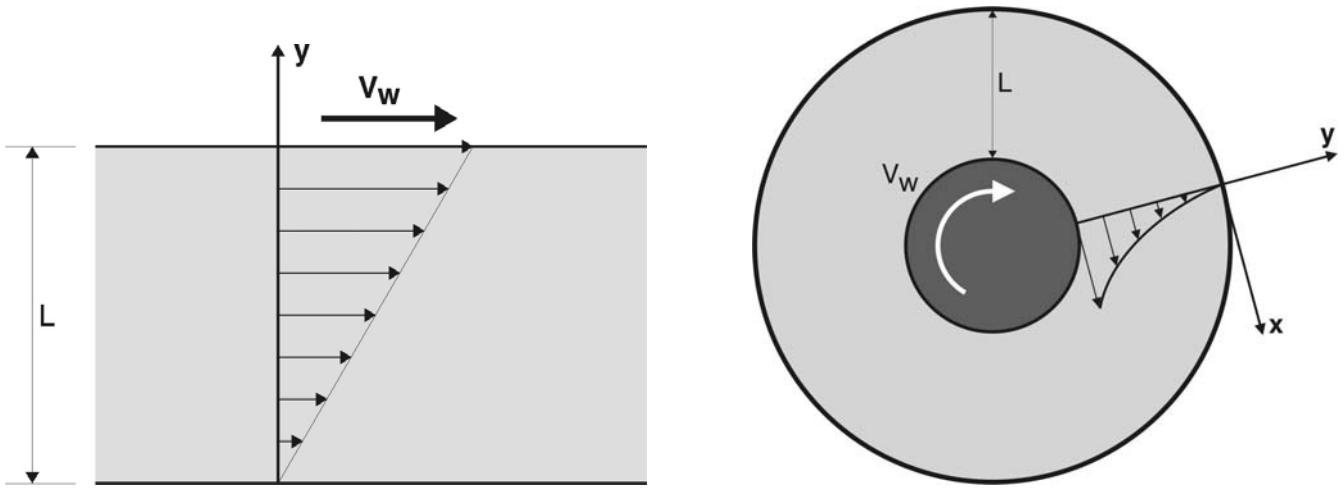


Figure 19 – Configurations of confined granular flows:
 (a) plane shear, (b) annular shear (after GDR-MiDi, 2004)

Figure 20a highlights the abrupt decrease of the volume fraction necessary to maintain a flowing condition when a critical shear straining rate is reached. In the case shown, the transition between quasi-static and collisional regime begins for an I value of approximately 0.15. Figure 20b clearly demonstrates the rate effect on the macroscopic friction, similar to those experimentally obtained by Randolph and co-workers, and shown in Figure 10.

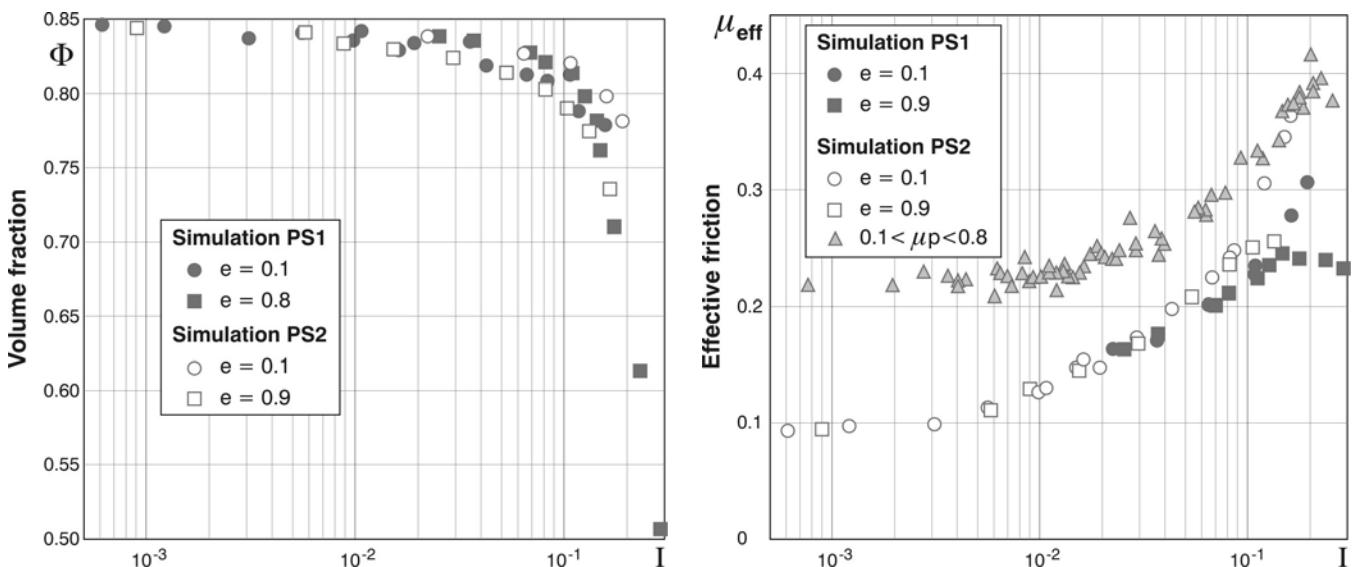


Figure 20 – Results of polydisperse disks and spheres simulations under plane shear:
 (a) Volume fraction and (b) effective friction vs. adimensional inertia (after GDR-MiDi, 2004)

Figure 21a highlights a most interesting hysteresis, akin to the difference observed in tribology between static and kinetic friction: a higher friction has to be overcome to initiate (up stress ramp) flow sliding, while the initiated flow can be maintained at a lower friction (down stress ramp). Figure 21b shows that the friction measured at the inner drum may be affected by only a few particles bounded by the inner drum.

Figure 22 maps out various flow regimes obtained by Campbell (2002) using 3-D DEM simulations of one thousand monodisperse spheres. The transition volume fractions are plotted vs. the Elastic to inertial shear stress ratio (θ factor). This description implies that the volume fraction is the key factor controlling the transition between the various regimes, with the non dimensional stiffness playing a secondary role. For rigid or slowly sheared grains ($\theta > 10^4$), the behaviour abruptly transitions from quasi-static to inertial within a couple of percent of the volume fraction, at approximately 0.59 (identical to Bagnold kinematic consideration for

dispersions). An additional nuance is introduced within the inertial regime, inasmuch the average contact time t_c between particles is compared to that of a purely binary contact time T_{bc} . The lower the actual contact time, the closer to a gas the medium behaves. For soft or rapidly sheared grains ($\Theta < 10^4$), an elastic-inertial regime can appear as a transition between quasi-static and inertial regimes.

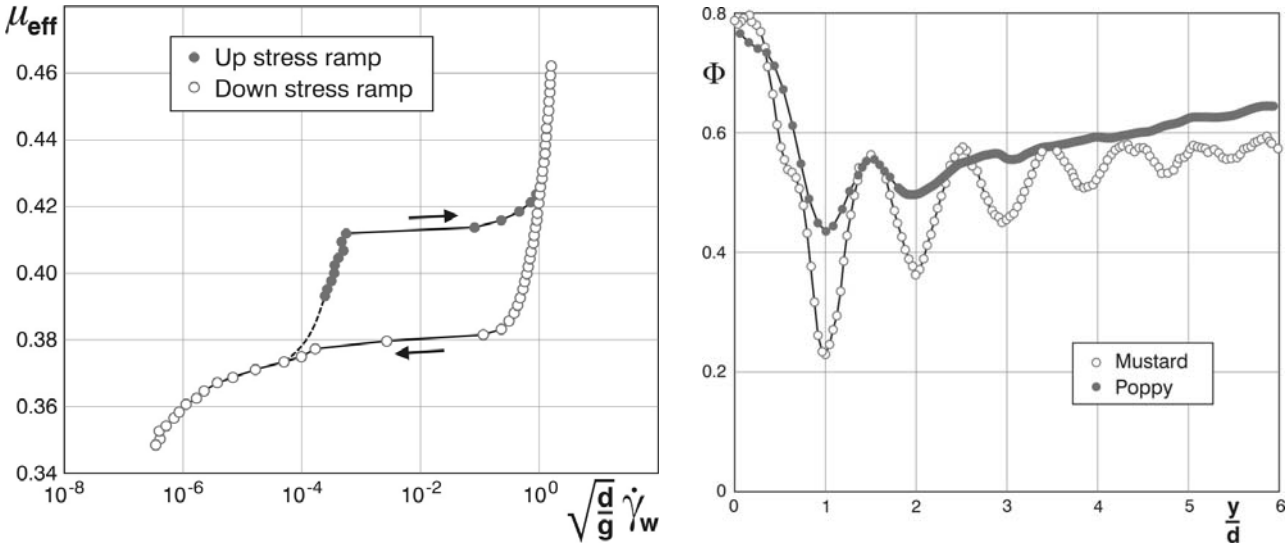


Figure 21– Results of monodisperse spheres annular shear experiments:
 (a) Effective friction for polystyrene beads vs. shear straining rate,
 (b) volume fraction radial profiles (after GDR-MiDi, 2004)

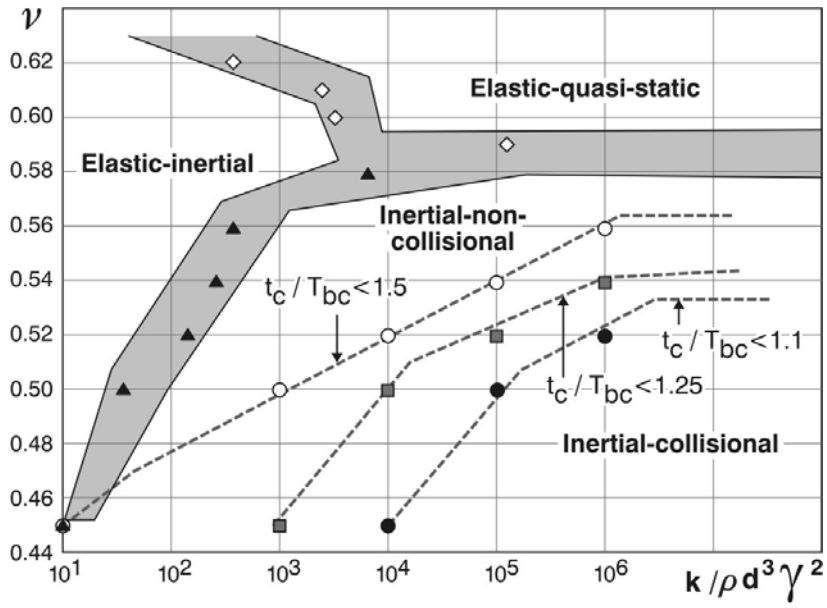


Figure 22 – Flowmap of various flow regimes for $e=0.7$ and $\mu=0.5$ (after Campbell, 2002)

5.3. Recent imaging and velocimetry techniques

Discrete elements can also be physically modelled in the laboratory. Howel et al (1999) have produced insightful images of an annular shear test, as shown in Figure 23a, using photoelasticity. One of the most impressive advances in the experimental study of granular media is the use of Magnetic Resonance Imaging (MRI), traditionally used for medical applications. Da Cruz (2004) has presented remarkable results provided by MRI equipment, shown in Figure 23b, of an annular shear test. Techniques specially developed for granular media (Raynaud et al., 2002) enable researchers in that case to develop velocity profiles.

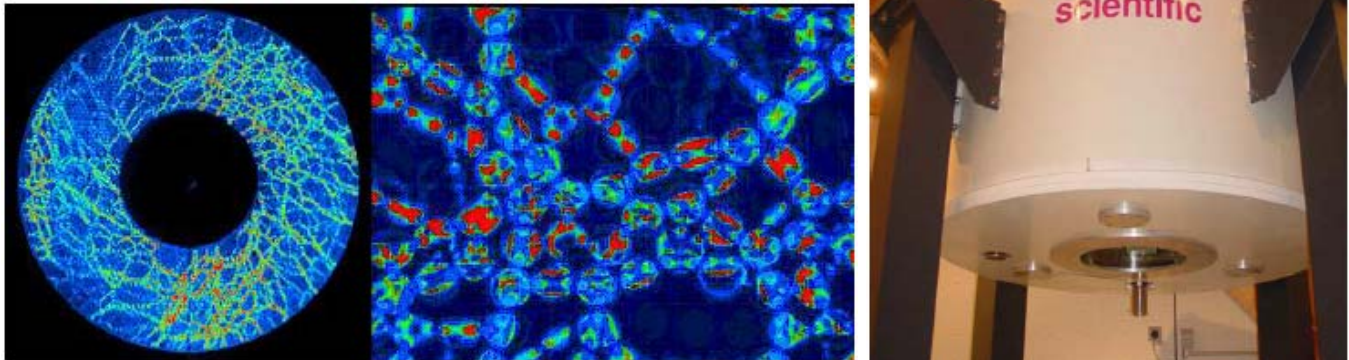


Figure 23. Results of annular shear experiments: (a) Photoelastic imaging of contact forces chains, (Howell et al., 1999) (b) Magnetic resonator of LMSGC at ENPC (Da Cruz, 2004)

6. Conclusion

The magic survives while scientists continue making progress. We will probably have to wait for another couple of generations before we can cast a comprehensive framework describing the various behaviour types of a mixture of grains, air and water, when agitated by a vibrator. Theoretical, experimental, and significant numerical resources will have to be combined to get to the bottom of the vibratory driving question.

7. Suggestions for further study

After reviewing several fundamental and applied aspects of vibratory driving and densification, the following suggestions for further consideration are offered :

- soil mechanics research is needed in combination with cousin disciplines in the area of large cyclic deformation to better understand and assess the effects of degradation and liquefaction under those extreme conditions,
- full scale vibratory driving tests, with extensive field monitoring, are to be preferred to reduced scale laboratory tests, which suffer from improper energy dissipation boundary conditions,
- potential and transferred power of vibrators need to be better defined, as well as modelled for better description of the mechanical behaviour of vibrators,
- peak vibration of the soil surrounding a profile upon vibrator start up does not necessarily imply soil resonance; it can also result from the combination of increasing frequency and degrading soil resistance,
- monitoring of vibrated profiles is recommended with the view to emulate the benefits accrued by a similar practice for driven profiles, and procedures for vibratory loading tests should be developed.

8. References

- Babic M., Shen H. H., Shen H. T. 1990 The stress tensor in granular shear flows of uniform,deformable disks at high solids concentrations. *J. Fluid Mech.* 219, 81-118.
- Bagnold R. A. 1954 Experiments on a gravity-free dispersion of large solid particles in a Newtonian fluid under shear. *Proc. R. Soc. Lond. A* 225, 49-63.
- Bauer E. (1996). "Calibration of a Comprehensive Hypoplastic Model for Granular Materials." *Soils and Foundations*, Vol. 36, N°1, pp.13-26.
- Barkan D.D., (1963), Méthodes de vibration dans la construction, Dunod, Paris, 302 p. (*French translation of Original in Russian "Vibrometod V Stroiteljstve*, 1960)
- BBRI .(1994). High performance vibratory pile drivers base on novel electromagnetic actuation systems and improved understanding of soil dynamics, *Progress reports of the BRITE/EURAM research contract CT91-0561*, 1994.
- Bernhard, R.K., (1967), Fluidization phenomena in soils during vibro-compaction and vibro-pile-driving and –pulling. Hanover, NH 1967, 58 pp., *US Army Cold Regions Research and Engineering*.
- Billet P., Sieffert J.G., (1989). "Soil-sheet pile interaction in vibro-piling" *Journal of Geotechnical Engineering*, ASCE, Vol. 115, N° 8, pp. 1085-1101
- Borel S. et al. (2002), "Full-scale behaviour of vibratory driven piles in Montoir", Proceedings of Transvib2002 Conference, Louvain-la-Neuve, Sept 9-10, 17 p.
- Campbell, C.S., (2002), *Granular shear flows at the elastic limit*, *J. Fluid Mech.* (2002), vol. 465, pp. 261-291.
- Chua K.M., Gardner S., Lowery L.L., (1987). "Wave Equation Analysis of a Vibratory Hammer-Driven Pile", *Proc. Offshore Technology Conf.*, Vol. 4, pp. 339-345
- Da Cruz F. (2004), "Ecoulement de grains secs: Frottement et blocage", These de Doctorat de l'Ecole Nationale des Ponts et Chaussees, Matériaux et Structures, ENPC, Paris, Version provisoire, 282 pp.
- Davisson M.T., (1970). "BRD Vibratory driving formula", *Foundation facts*, Vol. 1, N° 1, pp. 9-11
- Dayal U., Allen J.H. (1975) The Effect of Penetration Rate on the Strength of Remoulded Clay and Sand Samples. *Canadian Geotechnical Journal* 12, 336-348.
- Deveugle C., Mossoux G. (2006). « Modelisation de la dynamique des milieux granulaires », Travail de fin d'études, Département de Genie Civil et Environnemental, Université catholique de Louvain, Louvain-la-Neuve, 128 pp.
- Dobry R., Ladd R.S., Yokel F.Y., Chung R.M., Powell D. (1982). "Prediction of Pore Water Pressure Buildup and Liquefaction of Sands During Earthquakes by the Cyclic Strain Method". *National Bureau of Standards Building Science Series 138*, July 1982, 150 pp.
- Dobry R., Swiger W.F. (1979). "Threshold Strain and Cyclic Behavior of Cohesionless Soils". *Proc. 3rd ASCE/EMDE Specialty Conference*. Austin, Texas, pp. 521-525;
- Dobry R., Vucetic M. (1987). "State-of-the-Art Report: Dynamic Properties and Response of Soft Clay Deposits". *Proceedings of the Intl. Symposium on Geotechnical Eng. of Soft Soils*, Mexico City, Vol. 2, pp. 51-87.
- Drnevich V.P., Hall J.R., Richart F.E. (1967). "Effects of Amplitude of Vibration on the Shear Modulus of Sand." *Proceedings of the International Symposium on Wave Propagation and Dynamic Properties of Earth Materials*, Albuquerque, N.M., pp. 189-199.
- Dubois F., (2006) La plateforme LMGC90, cours, Université de Montpellier, LMGC.
- Finn W. D. L. (1981) "Liquefaction Potential: Developments Since 1976", *Proceedings, Intl. Conf. on Recent Advances in Geotechnical Earthquake Engineering and soil Dynamics*, St. Louis, Missouri, Vol. II, pp. 655-681.
- Gardner, Sherrill, (1987). "Analysis of vibratory driven pile". *Proc. of 2nd Int. Conf. on Deep Foundation*, Luxembourg, 5-7 May, pp. 29-56.
- GDR-MiDi (2004), « On dense granular flows », *Eur. Phys. J. E* 14, 341-365
- Geuzaine C., Remacle JF. « Gmsh Reference Manual ». Edition 1.34, janvier 2006.
- Gonin J. (1998), Quelques réflexions sur le vibrofonçage, *Revue Française de Géotechnique*, N° 83, 2^{ème} trimestre, pp. 35-39

- Grabe J., König F., Mahutka K.-P. (2006). Numerical modelling of pile jacking, driving and vibratory driving. *Numerical Modelling of Construction Processes, Bochum*, 235-246.
- Gudehus, G. (1996). "A comprehensive constitutive equation for granular materials." *Soils and Foundations*, Vol. 36, N° 1, 1-12.
- Hardin B.O., Black W.L. (1968). "Vibration Modulus of Normally Consolidated Clay." *Journal of the Soil Mechanics and Foundations Division, ASCE*, Vol. 94, No. SM2, Proc. Paper 5833, pp. 353-369.
- Holeyman A. (1985) "Dynamic non-linear skin friction of piles," *Proceedings of the International Symposium on Penetrability and Drivability of Piles*, San Francisco, 10 August 1985, Vol. 1, pp. 173-176.
- Holeyman A. (1988) "Modeling of Pile Dynamic Behavior at the Pile Base during Driving," *Proceedings of the 3rd International Conference on the Application of Stress-Wave Theory to Piles*, Ottawa, May 1988, pp. 174-185.
- Holeyman A. (1993a) "HYPERVIB1, An analytical model-based computer program to evaluate the penetration speed of vibratory driven sheet Piles", Research report prepared for BBRI, June, 23p.
- Holeyman A. (1993b) "HYPERVIBIIa, An detailed numerical model proposed for Future Computer Implementation to evaluate the penetration speed of vibratory driven sheet Piles", Research report prepared for BBRI, September, 54p.
- Holeyman A., Legrand C. (1994). Soil Modelling for pile vibratory driving, *International Conference on Design and Construction of Deep Foundations*, Vol. 2, pp 1165-1178, Orlando, U.S.A., 1994.
- Holeyman A., Legrand C., Van Rompaey D. (1996). A Method to predict the driveability of vibratory driven piles, *Proceedings of the 3rd International Conference on the Application of Stress-Wave Theory to Piles*, pp 1101-1112, Orlando, U.S.A., 1996.
- Holeyman A. E. Soil behavior under vibratory driving (2002). *Proceeding: International Conference on Vibratory Pile Driving and Deep Soil Compaction – Transvib 2002*, Louvain-La Neuve, 3-19.
- Houzé, C. (1994). HFV Amplitude control vibratory hammers : piling efficiency without the vibration inconvenience, in DFI 94, pp. 2.4.1 to 2.4.10, *Proceedings of the Fifth International Conference and Exhibition on Piling and Deep Foundations*, Bruges, Belgium, 1994.
- Howell, D. Behringer R.P., Veje C.T. (1999), "Stress fluctuations in a 2nd granular Couette experiment: a continuum transition. *Phys. Rev. Lett.*, 82 :5241-5244.
- Idriss I.M., Dobry R, Singh R.D. (1978). "Nonlinear Behavior of Soft Clays during Cyclic Loading." *J. Geotechnical Engineering Div., ASCE*, 104(GT12), pp. 1427- 1447.
- IREX (1998), Vibrofonçage des pieux et palplanches – Etude exploratoire, (by Le Tirant, P., Borel, S., Gonin, H., Guillaume, D. and Longueval, A.)
- Jean M. (1996) Documentation sur LMGC. Université de la Méditerranée.
- Jonker G., (1987). "Vibratory Pile Driving Hammers for Oil Installation and Soil Improvement Projects". *Proc. of Nineteenth Annual Offshore Technology Conf.*, Dallas, Texas, OTC 5422, pp. 549-560.
- Kondner R. L. (1963). "Hyperbolic Stress-Strain Response: Cohesive Soils." *Journal of the Soil Mechanics and Foundations Division, ASCE*, Vol. 89, No. SM1, pp. 115-143, Jan.
- Le Thiet, T., Canou J., Dupla J.-C. (2005) Etude du processus de vibrofonçage d'un pieu en chambre d'étalonnage, *Proc. 16th Int. Conf. on Soils Mech. and Geotech. Engineering*, Osaka, 12-16 Sept. Balkema, Vol. 2, 823-826
- Masing G. (1926), "Eigenspannungen und Verfestigung beim Messing", *Proceedings of Second International Congress of Applied Mechanics*, pp. 332-335.
- Midendorp P., Jonker G. (1988), Prediction of Vibratory Hammer Performance by Stress wave Analysis, *Preprint to the 3rd Int. Conf. on the Application of Stresswave Theory to Piles*, Ottawa
- Moulai-Khatir, Reda. O'Neill, Michael W., Vipulanandan C., (1994). "Program VPDA Wave Equation Analysis for Vibratory Driving of Piles", *Report to The U.S.A. Army Corps of Engineers Waterways Experiments Station. Dept. of Civil and Environmental Engineering*,

- UHCE 94-1, Univ. of Houston, Texas, August 1994, 187 pp.
- Niemunis A., Herle I. (1997) Hypoplastic model for cohesionless soils with elastic strain range. *Mechanics of Cohesive-Frictional Materials*, 4 (2), 279-299.
- Novak M., Nogami T., Aboul-Ella F. (1978). "Dynamic Soil Reactions for Plane Strain Case", *J. Engrg. Mech. Div., ASCE*, 104(4), 953-959.
- NRC (1985). "Liquefaction of Soils During Earthquakes." National Research Council Committee on Earthquake Engineering, Report No. CETS-EE-001, Washington, D.C.
- O'Neill Michael W., Vipulanandan C., (1989). "Laboratory evaluation of piles installed with vibratory drivers". *National Cooperative Highway Research Program*, Report n° 316, National Research Council, Washington, DC. Vol. 1 pp. 1-51. ISBN 0-309-04613-0
- O'Neill Michael W. Vipulanandan C., Wong D., (1990). "Laboratory modelling of vibro-driven piles". *Journal of Geotechnical Engineering, ASCE*, Vol. 116, N° 8, pp. 1190-1209
- Raynaud J.S., Moucheront P., Baudez J.C., Bertrand, F., Guilbaud, J.P., and Coussot, P. (2002), "Direct determination by nuclear magnetic resonance of the thixotropic and yielding behaviour of suspension, *J. Rheol.*, 46 :709.
- Reynolds O. (1885), "On the dilatancy of media composed of rigid particles in contact", *phil. Mag. Ser.*, 5(20) :469-481.
- Robertson P.K., Wride C.E. (1998). "Evaluating cyclic liquefaction potential using the cone penetration test", *Canadian Geotechnical Journal*, No. 35, pp. 442-459.
- Rodger A.A., Littlejohn G.S. (1980). "A study of vibratory driving in granular soils". *Geotechnique*, Vol. 30, n° 3, pp. 269-293.
- Seed H.B., Idriss I.M. (1970). "Soil Moduli and Damping Factors for Dynamic Response Analyses." Earthquake Engineering Research Center, College of Engineering, University of California, Berkeley, Report No. EERC 70-10.
- Seed H.B., De Alba P. (1986) "Use of SPT and CPT Tests for Evaluating the Liquefaction Resistance of Sands" *Proc. INSITU 86*, VA, 22 p.
- Schmid W.E., (1969). "Driving resistance and bearing capacity of vibrodriven model piles". *American Society of Testing and Materials Special Techn.*, Publ. 444, pp. 362-375
- Schmid W.E., Hill H.T. (1967). "A rational dynamic equation for vibro driven piles in sand". *Symp. Dynamic Properties of Earth Materials. New Mexico University*, p. 349.
- Smith E.A.L., (1960). "Pile-driving analysis by the wave equation". *Journal of the Soil Mechanics and Foundations Divisions, ASCE*, Vol. 86, August 1960.
- Vanden Berghe J-F, (2001) "Sand Strength degradation within the framework of pile vibratory driving", doctoral thesis, Université catholique de Louvain, Belgium, 360pages.
- Viking K., (1997). "Vibratory driven pile and sheet piles – a literature survey", *Report 3035, Div. of Soil and Rock Mechanics, Royal Institute of Technology, Sweden*, 75 p.
- Viking K., (2002). "Vibratory driven pile and sheet piles ", *PhD Thesis, Div. of Soil and Rock Mechanics, Royal Institute of Technology, Sweden*, 375 p.
- Vucetic M., Dobry R. (1988). "Degradation of Marine Clays Under Cyclic Loading. *ASCE Journal of Geotechnical Engineering*, Vol. 114, No.2, pp.133-149.
- Vucetic M., Dobry R. (1991). "Effect of Soil Plasticity on Cyclic Response." *ASCE Journal of Geotechnical Engineering*, Vol. 117, No. 1, pp. 89- 107.
- Vucetic M. (1993). "Cyclic Threshold Shear Strains of Sands and Clays", Research Report, UCLA Dept. of Civil Engineering, May 1993.
- Vucetic M. (1994). "Cyclic Threshold Shear Strains of Sands and Clays", Paper in print, *ASCE Journal of Geotechnical Engineering*
- Warrington Don. C., (1989). "Driveability of Piles by vibration". *Deep Foundations Institute 14th Annual members Conf.*, Baltimore, Maryland, USA, pp. 139-154.
- Westerberg E., Massarch K., Rainer Eriksson K., (1995). "Soil resistance during vibratory pile driving", *Proc. to Int. Symposium on Cone Penetration Testing*, Linköping, Sweden, Vol. 3, Report 3.41, pp. 241-250.
- Youd L.T. (1972). Compaction of sands by repeated shear straining, *Journal of the Soil Mechanics and Foundations Division*, 1972, Proc. ASCE, Vol. 98, SM7, pp. 709-725.